THE JOURNAL OF PHYSICAL CHEMISTRY A

Article

pubs.acs.org/JPCA

Raman Spectroscopy of Water–Ethanol Solutions: The Estimation of Hydrogen Bonding Energy and the Appearance of Clathrate-like Structures in Solutions

Tatiana A. Dolenko,*[,†] Sergey A. Burikov,[†] Sergey A. Dolenko,[‡] Alexander O. Efitorov,[†,‡] Ivan V. Plastinin,[†] Viktor I. Yuzhakov,[†] and Svetlana V. Patsaeva[†]

[†]Department of Physics and [‡]D. V. Skobeltsyn Institute of Nuclear Physics, M. V. Lomonosov Moscow State University, Moscow 119991, Russia

Supporting Information

ABSTRACT: The structure of aqueous alcohol solutions at the molecular level for many decades has remained an intriguing topic in numerous theoretical and practical investigations. The aberrant thermodynamic properties of water–alcohol mixtures are believed to be caused by the differences in energy of hydrogen bonding between water–water, alcohol–alcohol, and alcohol–water molecules. We present the Raman scattering spectra of water, ethanol, and water–ethanol solutions with 20 and 70 vol % of ethanol thoroughly measured and analyzed at temperatures varying from −10 to +70 °C. Application of the MCR-ALS method allowed for each spectrum to extract contributions of molecules with different strengths of hydrogen bonding. The energy (enthalpy) of formation/weakening of hydrogen bonds was calculated using the slope of Van't Hoff plot. The energy of hydrogen bonding in 20 vol % of ethanol was found the highest among all the samples. This finding further supports appearance of clathrate-like structures in water–ethanol solutions with concentrations around 20 vol % of ethanol.

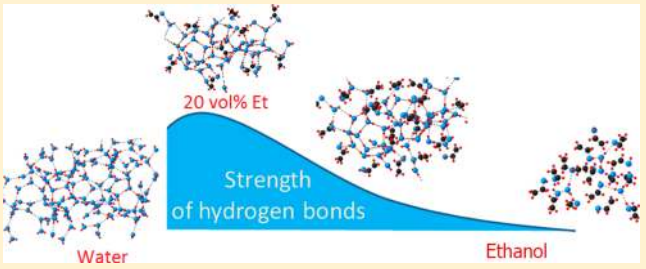

1. INTRODUCTION

The study of the structure of aqueous alcohol solutions is important from both theoretical and practical points of view.[1−4] Despite much research on these mixtures, the details of their molecular structuring has not yet been realized. Water–alcohol mixture represents a complex system in which the nature of the intermolecular bonds and interactions is not fully understood. It is well-known that physicochemical properties of water–alcohol solutions exhibit variety of anomalies over a wide range of composition. Many experimental studies have demonstrated that alcohol and water undergo incomplete mixing, resulting in a negative entropy of mixing.[5−8] Thermodynamic and transport properties of water–alcohol mixtures, such as negative excess partial molar volume of ethanol, diffusion coefficient, compressibility, viscosity, Walden product, excess sound absorption coefficient at low concentrations, etc., show considerable deviations relative to the ideal solution.[9−14]

There is a lot of scientific literature on the study of the structural features of water–ethanol solutions. However, sometimes conclusions in those publications are extremely controversial.[15] For example, some authors[6,16,17] claim that ethanol molecules in water–ethanol mixtures are found nearly in the same environment as in pure ethanol. Dixit et al.[6] explains the anomalous thermodynamic properties of alcohol solutions by incomplete mixing of alcohol and water rather than from water reorganization. They confirm using neutron diffraction that the concentrated alcohol–water mixtures with mole fraction of methanol 0.7 behave similarly to pure components in the mixture, and that the number of hydrogen bonds per molecule in the mixture does not deviate strongly from that in the pure solvents before mixing.[6] Nishikawa and Iijima as a result of study of water–ethanol mixtures by the method of small-angle X-ray scattering found that in these solutions there are no large clusters.[17] They state that clathrate-like clusters do not exist as a main component in water–alcohol solutions because the hydrogen bonding energy is nearly the same. Therefore, clusters are only transient and unstable. The authors also assert that the hydrophobic headgroups of ethanol are too small to form a stable cage, and the alkyl chain length of ethanol is too short to participate in stable interactions between clusters.[17] The results of studies of the dependence of HOH bending band (1600–1900 cm^{-1}) of water–ethanol solutions on the ethanol concentration allows us to assert that at low concentrations of ethanol in water–ethanol solutions ($x_{Et} < 0.03$) a network of water molecules is the same as in pure water.[18]

Such data interpretation contradicts the views of other authors describing water structure as more ordered near

Received: July 11, 2015
Revised: October 12, 2015

DOI: 10.1021/acs.jpca.5b06678
J. Phys. Chem. A XXXX, XXX, XXX−XXX

hydrophobic headgroups of the alcohol. The majority of experts came to the conclusion that, as a result of hydrophobic hydration in water−ethanol solutions, the self-organization of molecules is observed, resulting in formation of various molecular associates including clathrate-like structures.[1,2,4,19−42] The aberrant thermodynamic properties are explained by the structural features of water and alcohol mixtures, including different the strength of the hydrogen bond between water−water, alcohol−alcohol, and alcohol−water molecules. The problem lies in understanding how hydrophobic interactions between the alkyl headgroups of alcohol molecules as well as hydrogen bonding between the hydroxyl groups of water and alcohol molecules "help" each other to create various structural associates in the mixtures.

Many theoretical calculations indicate the existence of stable water−ethanol complexes in water−ethanol solutions.[1,19−28] The calculations of Matsugami et al.[1] of hydrogen bonding in water−ethanol solutions using the method of molecular dynamics showed that at the mole fraction of ethanol $x_{Et} \approx 0.20$ the hydrogen bonds in solution increase. To explain the anomalous negative excess entropy of mixing ethanol and water, Soper et al. proposed the clustering model.[19,20] This model supposes the formation of clusters of water molecules in the presence of alcohol component in the whole range of ethanol solubility. By theoretical analyses and computer simulations it was shown that the anomalous properties of water−ethanol solutions emerge from the appearance of a bicontinuous phase occurring at a relatively low mole fraction of ethanol $x_{Et} \approx 0.06−0.10$ (that amounts to a concentration of 17−26 vol %, which is a wide range).[21] Murthy[21] theoretically showed that the hydroxyl groups of ethanol behave as both proton donors and proton acceptors. As a result, there is a considerable probability of simultaneous hydrogen bonding between oxygen and hydrogen atoms with different cages of water molecules.

The presence of associates in water−ethanol solutions is evidenced by many experimental data.[2,4,29−42] Li and co-workers[2] used PFG-NMR as well as terahertz techniques to study transitions in the structuring of binary alcohol/water solutions. For three critical mole fractions of ethanol (0.07, 0.15, 0.60 mol) they demonstrated that at $x_{Et} \approx 0.15$ the greatest nonideality of the liquid structure exists and the extended hydrogen bonded networks between alcohol and water molecules are formed. Mizuno et al.[29] performed ^{1}H NMR, ^{13}C NMR, and FTIR studies of water−ethanol solutions with different contents of ethanol and temperatures and showed that in solutions with ethanol content up to $x_{Et} = 0.60$ mol the bonds between the water molecules surrounding the ethanol alkyl group become stronger. At higher alcohol concentrations the hydrogen bonds between the hydrogen atom of water and the oxygen atom of the hydroxyl group of self-organized aggregates of ethanol become stronger. Similar results were found by Matsumoto et al.[33] Using the methods of X-ray diffraction and mass spectrometry, they showed that in the ethanol concentration range $0.20 < x_{Et} < 0.80$ the so-called polymer hydrates of ethanol exist in water−ethanol mixtures. The fundamental structure of those ethanol hydrates is unchanged, and the majority of water molecules is not bonded with each other and serves as stabilizer in polymer ethanol hydrates.

Nishi and co-workers[36] used IR spectroscopy to study the formation of hydrogen bonding clusters of molecules of water and alcohol in diluted water−ethanol solutions ($x_{Et} < 0.03$) near ambient temperatures. Also, they carried out the analysis of clusters using mass spectrometry and X-ray diffraction. The IR spectroscopy results indicated that even in dilute solutions the association of dissolved substances occurs. Nishi et al. described the observed results in terms of a "clathrate structure" with a hydrophobic core composed of coherent ethyl groups with a hydrogen bonding water cage.[36]

Other concepts of the structure of water−ethanol solutions also exist in the scientific literature. The Raman spectra in the low-frequency region of the water−ethanol binary mixtures with different proportions can be decomposed into linear combination of the partial spectra representing pure ethanol and pure water.[34] According to these results,[34] ethyl alcohol and water at the molecular level do not get ideally mixed, and the hydrogen bonds between ethanol associates and water associates are weak; thus, authors propose cluster model of ethanol molecules resembling a double-layer sandwich stacked by hydrophobic interaction.

Juurinen and co-workers[38] applied the Compton scattering technique using synchrotron X-rays to study the structure of ethanol/water mixtures. The experiments showed two apparently distinct in terms of geometry mixing regimes: the dilute one with $x_{Et} = 0.05$ and the concentrated regime with $x_{Et} > 0.15$. The authors believe that their results confirm the hypothesis of clathrate-like structures at dilute concentrations of ethanol in water.

The analysis of literature data shows that many experimental[1,7,10,14,27,33,34,36,37,39−42] and theoretical[21,27] results point out the existence of the singular point at a certain alcohol concentration (in ethanol it occurs for molar fraction around $x_{Et} \approx 0.20$ at ambient temperatures), dividing the states with quite different molecular configurations. In the water-rich region at ethanol concentration $x_{Et} < 0.01$, the tetrahedral-like network of hydrogen bonds of water molecules is mostly preserved. Water molecules surround single ethanol molecules creating hydrogen bonds with hydroxyl groups of ethanol. Due to hydrophobic interactions with the increasing concentration of ethanol the self-organization of water molecules occur.[1,4,7,10,14,21,27,33,34,36−42] According to the data of some authors,[1,14,21,36,39−42] at a certain concentration of ethanol up to the singular point $x_{Et} = 0.20$ there is significant strengthening of hydrogen bonds resulting in formation of clathrate-like structures, i.e., structures with the strongest hydrogen bonds. In the ethanol content range of $0.20 < x_{Et} < 1$ the clusters of sandwich-like structure prevail in ethanol−water solutions.[33,36]

Earlier, the authors of this work have carried out the studies of the dependence of vibrational spectra of water−ethanol mixtures on the concentration of ethanol using a combination of Raman scattering and IR absorption spectroscopy.[39−42] We investigated water−ethanol mixtures with various concentrations spreading from water until pure ethanol. The spectral contour survey of a wide stretching band of OH vibrations along with increasing ethanol concentration revealed changes in hydrogen bonding in the mixtures. In the resolved spectra we observed four individual components; two of them are almost identical to vibrational spectra of pure water and pure ethanol. However, two other individual spectra resolved by MCR-ALS, differed in shape from the spectra of aqueous ethanol solutions. We assumed that these resolved spectra represented two ethanol hydrates. The ratio of integral intensities in CH to OH vibrations in resolved spectra let us estimate composition of ethanol hydrates. The spectrum for the first, water-rich hydrate demonstrated a higher ratio of low-frequency (~3200 cm^{-1}) to

DOI: 10.1021/acs.jpca.5b06678
J. Phys. Chem. A XXXX, XXX, XXX−XXX

high-frequency (~3450 cm^{-1}) intensities compared to that of water. Because the low-frequency region within OH stretching band corresponds to vibrations of OH groups with strong hydrogen bonding, and the other spectral region is caused by the vibrations of weakly H-bonded OH groups, we concluded that hydrogen bonding between water molecules in water-rich hydrate has been strengthened compared to that of pure water. Moreover, the band shape of the OH stretching band in the resolved water-rich hydrate was found similar to the band shape of water in the Raman spectrum for a solid gas clathrate of structure II.[43] In contrast to water-rich hydrate, another ethanol hydrate showed weakened hydrogen bonding compared to the case for pure water.

Furthermore, we used the multivariate curve resolution-alternating least squares (MCR-ALS) analysis[44−47] and deconvolution of the OH Raman stretching band with the optimization method of genetic algorithm (GA)[48] to confirm our conclusions. According to our results, the behavior of the OH stretching band in both the Raman scattering and IR absorbance spectra along with rising ethanol content in the mixture demonstrated that the hydrogen bonding in the binary mixture with an ethanol concentration around 20 vol % (x_{Et} = 0.07) is stronger compared to that of pure water. At higher concentrations of ethanol (x_{Et} > 0.20), the strengthening of hydrogen bonding is gradually decreasing. The accurate MCR-ALS components analysis revealed the following components, giving the main contribution to the dependences of vibrational spectra of water−ethanol binary solutions versus concentration: water clusters, water-rich hydrate $EtOH{\cdot}5H_2O$, ethanol-rich hydrate of composition $EtOH{\cdot}1H_2O$ - $EtOH{\cdot}2H_2O$, and ethanol clusters.

On the base of the data of many authors, we consider the results obtained in the papers[39−42] as the confirmation of the hypothesis about the existence of clathrate-like structures in water−ethanol solutions at certain concentrations of ethanol. Here we use the term clathrate-like to describe the network of water molecules surrounding small nonpolar groups or molecules with enhanced hydrogen bonging among water molecules that can be disrupted by kinetic effects (for example, raised temperature). In the present paper we give the results of a thorough study of the temperature dependences of Raman spectra of water−ethanol solutions with certain ethanol content x_{Et} = 0 (pure water), 0.07 (20 vol %), 0.39 (70 vol %) and 0.85 (96 vol %), further supporting the hypothesis of the clathrate-like structures of a water network with enhanced hydrogen bonding at the ethanol concentration around x_{Et} = 0.07 (20 vol %) compared to that of pure solvents.

2. EXPERIMENTAL METHODS AND DATA PROCESSING

2.1. Objects of Research. Deionized bidistilled water with specific electrical conductivity 0.1 μSm/cm, ethanol (96%, Sigma-Aldrich), and water−ethanol solutions with ethanol concentrations of 20 and 70 vol % (that corresponds to molar fractions x_{Et} = 0.07 and x_{Et} = 0.39, accordingly) were used as objects of research. Such samples were chosen to verify the hypothesis of existence of clathrate-like structures in binary solutions: at 20 vol % of ethanol, the water network might contain structures similar to that in solid clathrates showing enhanced hydrogen bonding between water molecules, and at 70 vol % of ethanol the structure of water network in ethanol hydrates should differ from clathrate-like water structures (see Introduction).

2.2. Laser-Based Raman Spectrometer. The laser-based spectrometer was adjusted to measure Raman scattering spectra of all samples placed in the quartz cell. Raman spectra were excited by the radiation of the argon-ion laser operating at wavelength 488 nm and output power 300 mW. For suppression of elastic scattering, the edge-filter (Semrock) was used. It allowed measurement of spectra close by 100 cm^{-1} to the laser excitation frequency. The registration system consisted of the monochromator (Acton, grades 900 and 1800 g/mm, focal length 500 mm) and CCD-camera (Jobin Yvon, Synapse 1024*128 BIUV-SYN) and performed registration of spectra in a parallel detection mode. The practical spectral resolution was better than 1.0 cm^{-1}.

2.3. System of Sample Thermostabilization. To measure and maintain the temperature of liquid samples, the special stabilization system KRIO-VT-01 was used. Alteration and control of samples temperatures in a wide range from −30 °C up to +100 °C was performed with accuracy better than 0.1 °C. The supercooled state of liquid water within the cell volume of 3 × 3 × 30 mm^3 was reached at temperatures down to −10 °C.

2.4. Data Processing. The temperature dependences of Raman spectra for water, ethanol, and aqueous ethanol solutions in the temperature range from −10 °C (supercooled water and solutions) up to +70 °C were investigated. Polarized Raman spectra ($P_{||}$) were registered within the wavenumber range from 100 to 4000 cm^{-1}. Processing of the spectra included correction for the laser power, channel, and spectral sensitivities of the detector and intensity normalization by the total intensity of the stretching bands of CH and OH groups in the range 2500−4000 cm^{-1}.

To analyze the structure of Raman scattering bands, the method of multivariate curve resolution (MCR) was used.[44−47]

3. RESULTS AND DISCUSSION

3.1. Study of Temperature Dependence of Raman Spectra for Water−Ethanol Solutions. Figures 1−3 and Figure S1 show the obtained polarized Raman spectra of water, ethanol, and water−ethanol solutions at different temperatures. The behavior of the Raman stretching band of water with a temperature is similar to the data obtained by many authors.[49−52]

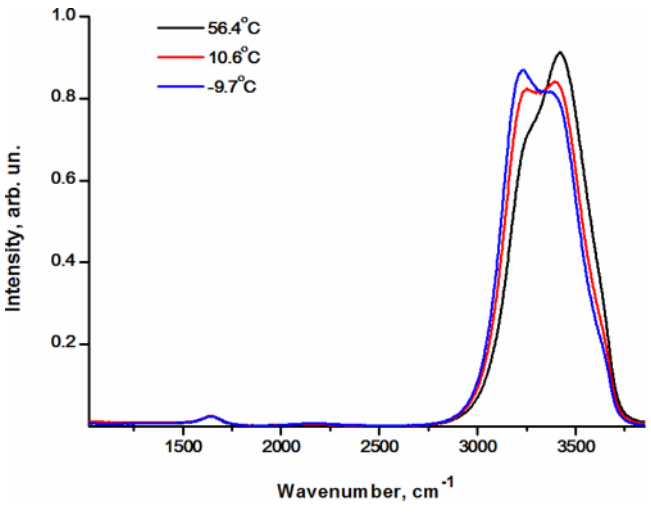

Figure 1. Polarized Raman spectra of water at different temperatures.

DOI: 10.1021/acs.jpca.5b06678
J. Phys. Chem. A XXXX, XXX, XXX−XXX

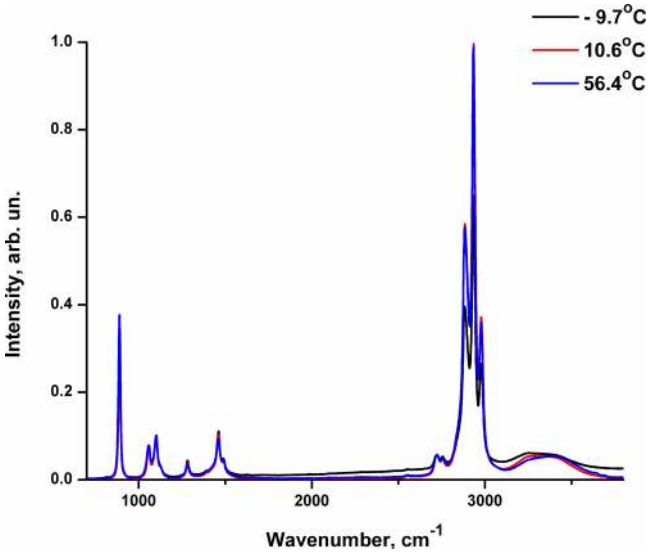

Figure 2. Polarized Raman spectra of ethanol at different temperatures.

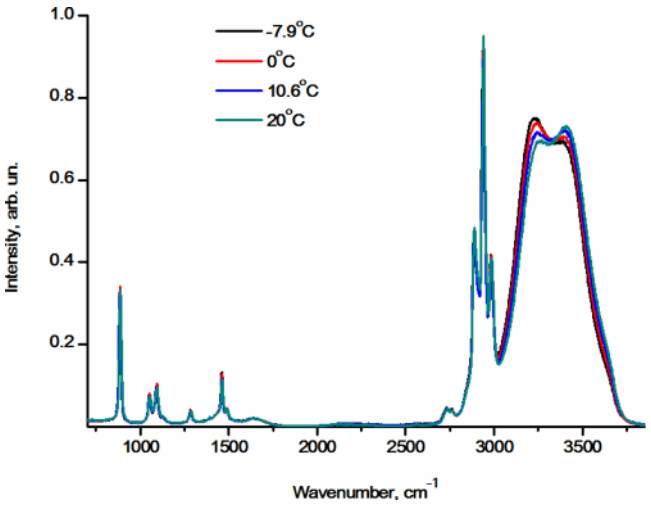

Figure 3. Polarized Raman spectra of 20 vol % water−ethanol solution at different temperatures.

The analysis of temperature dependences of Raman spectra of ethanol and water−ethanol solutions with ethanol concentrations of 20 and 70 vol % showed that the position and shape of the bands of C−H, C−O, and C−C vibrations remained constant upon variation of temperature (Figures 2 and 3). The temperature effect in the OH stretching band of aqueous ethanol is similar to that of the water stretching band (Figures 2 and 3).

The experimentally obtained spectra were used for quantitative estimation of the enthalpy of formation/weakening of the hydrogen bonds in water and water−ethanol solutions using the following approach. The Van't Hoff equation relates the standard enthalpy change and the equilibrium constant of reaction in the isobaric process:

$$\frac{\mathrm{d}\ln(k)}{\mathrm{d}T} = \frac{\Delta H^{\circ}}{RT^2} \quad \text{or} \quad \ln(k) = -\frac{\Delta H^{\circ}}{R}\cdot\frac{1}{T} + \text{const}$$

where k is the equilibrium constant of the reaction, T is the temperature, R is the universal gas constant, and ΔH° is the change of enthalpy during formation of one mole of hydrogen bonded molecules from nonbonded ones in their standard states under conditions of 298 K and 1 atm. Equilibrium constant of the reaction in this case is the concentration ratio of hydrogen bonded and nonbonded molecules.

Thus, to evaluate the enthalpy of formation/break of hydrogen bond it is necessary to find the mole ratio of molecules with strong and weak hydrogen bonds. Such a wide range of temperatures used, from supercooled to strongly heated samples, was chosen to provide higher contrast in strengthening of hydrogen bonds and, therefore, to achieve better accuracy of its energy calculation.

To select the contributions of molecules with strong and weak hydrogen bonds into vibrational spectra, the spectral contours were resolved into components using the method of multivariate curve resolution (MCR).[44−47] This method was chosen because of its lower degree of user bias in comparison with the other methods of decomposition into components, because it does not require any a priori assumptions about the number and shape of the components.[44,45]

3.2. Calculation of the Enthalpy of Formation/Weakening of Hydrogen Bonds in Water−Ethanol Solutions Using the Method of Multivariate Curve Resolution. Multivariate methods are very powerful mathematical instruments aimed at resolving multicomponent mixtures and at describing their evolution. The technique of extracting information from chemical systems using data-driven methods is called chemometrics. One of chemometric algorithms, multivariate curve resolution (MCR), is a model-free method targeted to describe the evolution of the results of experimental multicomponent measurements in terms of contributions of pure components, which are themselves unknown *a priori*.[44,45] Multivariate curve resolution-alternating least squares (MCR-ALS) is a version of MCR method that solves the MCR basic bilinear problem using a constrained alternating least squares algorithm.

The essence of the MCR method is decomposition of the experimental data matrix **D** (the array of spectra of the mixture in different conditions or at different time moments, in our case, Raman spectra of water, ethanol, and water−ethanol solutions at different concentrations) into a matrix product of the matrix **C** of pure concentration profiles of components and the transposed matrix $\mathbf{S}^{\mathrm{T}}$ of pure spectra of components: $\mathbf{D} = \mathbf{C}\mathbf{S}^{\mathrm{T}} + \mathbf{E}$. The matrix of residuals **E** is minimized during the decomposition. Linear operation assumes that there is no interaction among the components, and that at each moment/concentration the total spectrum of the mixture is a linear combination of initial spectra of the components, which remain unchanged, with variable weighting coefficients in the linear combination.

The number of possible different decompositions of the matrix **D** is very large. In the ALS (alternate least squares) algorithm, selection of one of them is performed by alternatingly determining one of the matrices **C** and **S** from the other one and matrix **D**, applying non-negativity constraint for both the spectra and concentration profiles (negative values in the obtained spectrum or concentration profile are changed to zero). In some cases, also unimodality and closure constraints are applied.[44] The decomposition is repeated until the minimum of the decomposition error is obtained. Due to use of only such very general and natural constraints, the obtained decomposition reveals the objective properties of the studied object, and it does not depend on the will of the scientist.

DOI: 10.1021/acs.jpca.5b06678
J. Phys. Chem. A XXXX, XXX, XXX−XXX

MCR is a powerful data analysis tool that still undergoes theoretical developments and finds new applications. For example, the MCR-ALS method has been used to study molecular clustering in alcohol solutions: MCR-ALS analysis with three and four components has been used to resolve the vibrational Raman scattering and IR absorbance spectra composed of overlapped bands, and to determine the composition of ethanol hydrates.[39−41] It has been also demonstrated that the MCR-ALS method could be successfully used for hyperspectral image resolution in remote sensing[46] and for understanding spectroscopic data from micellization-induced liquid−liquid fluctuations in of surfactants solutions in water.[47]

3.2.1. Calculation of the Enthalpy Change during Formation/Weakening of Hydrogen Bonds in Water. In our studies, in the first instance the MCR-ALS method was used to analyze water Raman spectra (100−4000 cm^{-1}) obtained in the temperature range from −10 up to +70 °C. The best accuracy was obtained by decomposition of water spectra into two components. Because we were interested in quantification of water molecules with strong and weak hydrogen bonds, we considered only the OH stretching band. Figure 4 shows the

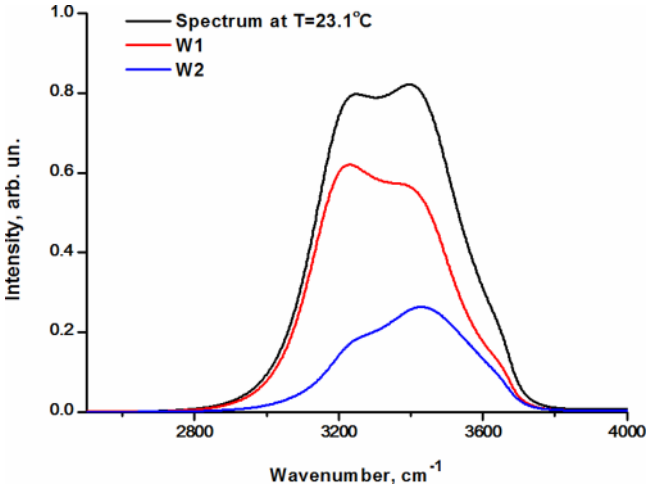

Figure 4. Water Raman OH stretching band at temperature 23.1 °C and its decomposition into two components by the MCR-ALS method.

Raman OH stretching band of water at temperature 23.1 °C and its decomposition by the MCR method into two components. Figure 5 shows the dependence of mole fractions of each component on water temperature.

This decomposition can be explained by the simplified model which assumes that in water there are two types of molecules: mostly with strong (type W1) and weak (type W2) hydrogen bonds. We slightly oversimplified the situation because both contours of individual spectral components W1 and W2 have a complex shape demonstrating "shoulders" around 3650 cm^{-1}, indicating the presence of OH groups with nearly broken hydrogen bonds. At the same time, we do not aim to interpret the topology of the associates of different types of water molecules. Perhaps similar types of molecules (type W1 or W2) could form isolated clusters with hydrogen bonds broken at the boundary of a cluster. Either equal water molecules represent associations resembling branched polymer chains with hydrogen bonds broken at the terminal points, and the associations of W1-molecules and W2-molecules can penetrate into each

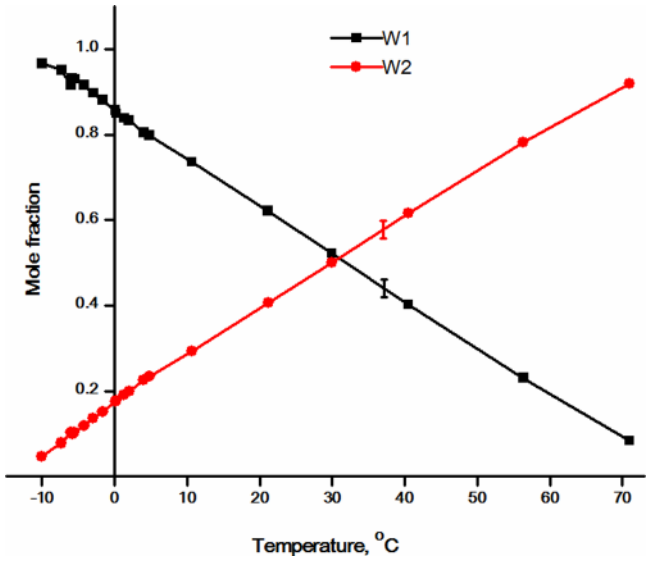

Figure 5. Temperature dependence of mole fractions of individual components resolved from water Raman OH stretching band.

other. Doubtlessly, the hydrogen bonds are not "frozen" in time, they are permanently broken and re-formed, and the water molecules are constantly switching from one type to another.[33]

The higher-frequency spectral component corresponds to the ensemble of molecules with weak bonds (the type W2), lower-frequency component corresponds to the ensemble of molecules with stronger bonding (the type W1). In this work it is assumed that the two components W1 and W2 have the same scattering cross-section. This supposition is based on the fact that square of water Raman valence band[52] and total square of Raman valence bands of OH and CH groups in water−ethanol solutions[42] practically do not change in the studied temperature region. The area ratio for these spectral components corresponds to the mole fraction ratio of molecules with strong and weak hydrogen bonds. The equilibrium constant in this case is also equal to the ratio of the areas under these individual components in resolved Raman spectrum.

The equilibrium constant k was calculated as a function of water temperature, and the Van't Hoff plot was constructed as a linear dependence of $\ln(k)$ on the inverse temperature (Figure S4a). The enthalpy of formation/weakening of hydrogen bonds between water molecules determined from the slope of the Van't Hoff plot is equal to $\Delta H^{w} = -21.4 \pm 0.7$ kJ/mol.

There are several approaches to characterize the strength of hydrogen bonds. The main criterion is the energy of hydrogen bonding. The energy of formation of strong hydrogen bonds could reach 15−20 kJ/mol or more in different substances. These include O−H···O in water, alcohols, carboxylic acids and O−H···N, N−H···O, and N−H···N in compounds containing hydroxyl, amide, and amine groups, such as proteins. Weaker hydrogen bonds have energies less than 15 kJ/mol. The lower limit of the hydrogen bond energy is 4−6 kJ/mol, for example, of the C−H···O in ketones, ethers, and aqueous solutions of organic compounds.[53] It should be noted that there are no direct methods for determining the energy of hydrogen bonds. Moreover, there is no standard definition for the energy of hydrogen bonding.[51,54] Therefore, estimations of hydrogen bond energy or enthalpy vary in different investigations. The

DOI: 10.1021/acs.jpca.5b06678
J. Phys. Chem. A XXXX, XXX, XXX−XXX

energy of attraction between molecules in liquid water has been estimated as 23.3 kJ/mol.[55] That is the energy required to break and completely separate the water molecules. The weakening of intermolecular bonds in liquid water from ~23 to ~17 kJ/mol under pressure at 200 °C was found when the majority of hydrogen bonds were broken in superheated liquid water losing the cooperativity.[56] Stokely et al. considered tetrahedral structures of bonded molecules with simultaneous hydrogen bonding and van der Waals interactions, the value for the directional component of the hydrogen bond he estimated as ≈12.0 kJ/mol.[57] The average thermal energy required to break hydrogen bonds in an ice-like, locally symmetric, strongly hydrogen bonded water claster was estimated from the temperature dependence of the oxygen K-edge X-ray absorption spectra as 6.3 kJ/mol in both liquid and solid state water.[58] Other experimental estimates made from Raman scattering spectra show that breaking the directional component of the hydrogen bond requires from 3.6 kJ/mol (weak bonds) to 20 kJ/mol (strong linear bonds).[59]

We presume that the value of the enthalpy change during formation/weakening of hydrogen bonds in water obtained in our experiments is in a good agreement with literature data.

3.2.2. Calculation of the Enthalpy Change during Formation/Weakening of Hydrogen Bonds in Water–Ethanol Solutions. Employment of MCR-ALS method to the temperature dependence of Raman scattering spectra of aqueous solutions with 20 or 70 vol % of ethanol demonstrated that these spectra are best described by four individual components. Figures 6 and 7 present the results of the

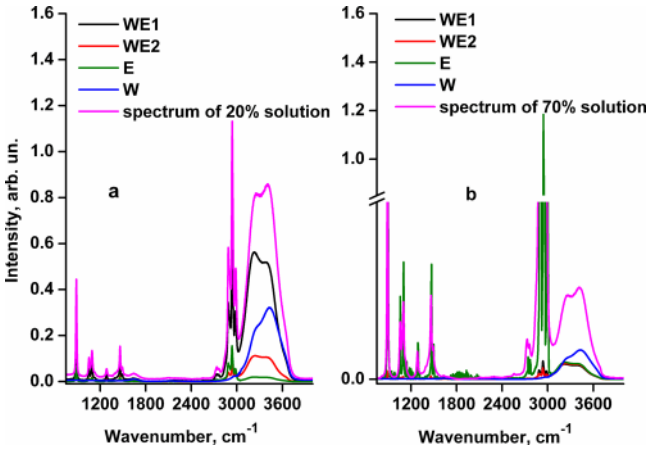

Figure 6. Raman spectrum for 20 vol % ethanol solution (at temperature 20.3 °C) (a) and for 70 vol % ethanol solution (at temperature 20.4 °C) (b) and their decomposition into four individual components by MCR-ALS method.

decomposition of Raman spectra of 20 vol % (Figures 6a and 7a) and 70 vol % (Figures 6b and 7b) aqueous ethanol in the studied temperature region. Figures S2 and S3 show the decomposition of the Raman spectrum for 20 vol % ethanol solution (Figure S2a–c) and for 70 vol % ethanol solution (Figure S3a–c) at the other temperatures into 4 individual components by MCR-ALS method.

As seen from the Figures 6 and 7, there are four components, WE1, WE2, E, and W, contributing to the Raman spectrum of water–ethanol solution with concentrations of ethanol of 20 and 70 vol %. The band shape of each component in the region of CH and OH stretching bands allows assuming that the

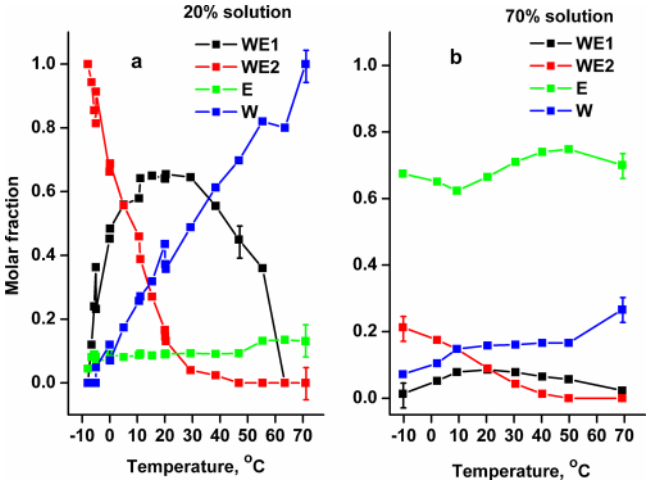

Figure 7. Temperature dependence of mole fractions of individual spectral components resolved from Raman spectra of 20 vol % ethanol (a) and from Raman spectra of 70 vol % ethanol (b).

component W corresponds exclusively to water molecules (there are no CH vibrations) and the component E corresponds to the ethanol molecules (the intensity of CH vibrations prevails). The components WE1 and WE2 contain intensive lines for both CH and OH stretching vibrations. From comparison of the intensities of the stretching bands of CH and OH groups and the width of the valence band of OH groups in the spectra of WE1 and WE2 components it follows that the associates WE1 and WE2 contain a significant amount of CH and OH groups of ethanol and water, connected by hydrogen bonds. Spectra of components WE1 and WE2 differ by the ratio of the intensities of these bands too. For example, the intensity of the CH bands (Figure 6a) shows that at temperature 20.3 °C the component WE1 contains many more CH groups than the WE2 component. And the ratio of the intensities of the stretching bands of CH and OH groups shows that ethanol hydrates contain different numbers of water molecules in hydrated shells: the ethanol hydrate WE1 contains a smaller number and the ethanol hydrate WE2 contains a larger number of water molecules.[39−42]

One should note that the MCR method did not make further decomposition of component W into constituents of W1 and W2 type as was done for pure water. It can be explained by the following way: distribution of hydrogen bonds by energy in water differs to a great extent from distribution in water component W. This distribution for component W is much narrower and that is why it causes no substantial contribution of difference between weak and strong hydrogen in the intensity of the valence band of OH groups.

In the proposed method of calculation of the enthalpy change during the formation/weakening of hydrogen bonds in the ethanol hydrates, the equilibrium constant is equal to the ratio of the total area under both spectral components WE1 and WE2 (corresponding to both types of ethanol hydrates), to the intensity of the component W (corresponding to water). Similar to the procedure described above for water, the enthalpy change during the formation/weakening of hydrogen bonds in the ethanol hydrates was calculated from the Van't Hoff plot as $\Delta H^{20\%} = -24.5 \pm 0.8$ kJ/mol.

In an analogous manner, the decomposition of Raman spectra of water–ethanol solution with 70 vol % of ethanol was performed by the MCR-ALS method. The results provided the

DOI: 10.1021/acs.jpca.5b06678
J. Phys. Chem. A XXXX, XXX, XXX–XXX

same spectral components (WE1, WE2, E, W) with small contents of component E (ethanol). The calculation of the enthalpy change during the formation/weakening of hydrogen bonds in the ethanol hydrates gave the value $\Delta H^{70\%} = -16.2 \pm 0.8$ kJ/mol.

The obtained values of the enthalpy of formation/weakening of hydrogen bonds characterize the average energy of hydrogen bonds in associates (both ethanol−water and water−water hydrogen bonds). Using the MCR component, it is impossible to separate ethanol−water hydrogen bonds from water−water hydrogen bonds in the associates. Thus, our estimations of the enthalpy of formation/weakening of hydrogen bonds in water and in water−ethanol solutions with concentrations of ethanol of 20% and 70% using Raman spectroscopy and MCR analysis showed that in a mixture with an ethanol concentration of 20%, the hydrogen bonds (both ethanol−water and water−water hydrogen bonds) are stronger than in pure water and ethanol and than in water−ethanol solution with an ethanol concentration of 70%.

The authors are not aware of studies in which the values of the enthalpy of formation/weakening of hydrogen bonds in ethanol hydrates in solutions with different ethanol concentrations were determined.

3.2.3. Calculation of the Enthalpy Change during Formation/Weakening of Hydrogen Bonds in Ethanol. The fact that the intensity of the OH stretching band in the Raman spectrum of 96% ethanol was small did not allow us to apply the approach of MCR-ALS spectral decomposition to the case of ethanol. Therefore, the calculation of the enthalpy of formation/weakening of hydrogen bonds in 96% ethanol was made on the base of temperature dependence of low-frequency ethanol Raman lines in a way similar to the method proposed by Edwards et al.[60] To calculate the equilibrium constant in ethanol, the authors used the low-frequency Raman line with maximum located at 270 cm^{-1} caused by intermolecular vibrations of neighboring molecules bonded by hydrogen bonds.[60] Therefore, the intensity of this band is determined by the concentration of exclusively hydrogen-bonded ethanol molecules. The other line with a maximum at 880 cm^{-1} is caused by vibrations of intramolecular C−C bonds in all ethanol molecules, either hydrogen-bonded through the hydroxyl group or not. Thus, the ratio of the intensities of the bands with maxima at 270 and 880 cm^{-1} allows determining the equilibrium constant k in ethanol. Drawing the Van't Hoff plot of $\ln(k)$ versus the inverse temperature and using its linear approximation one can determine the value of ΔH^{Et}.

In this study the Raman spectra of ethanol were obtained in the temperature range from −10 up to +70 °C. To determine the equilibrium constant k of ethanol, we used the intensities of the bands of intermolecular vibrations of neighboring molecules of ethanol and water bonded by hydrogen bonds with maximum at 270 cm^{-1} and of intramolecular vibrations of C−C of ethanol molecules at 886 cm^{-1} (Figure 8).

The observation of the low-frequency region of Raman spectra is connected with difficulties of extraction of useful signal from the background of strong elastic scattering (Rayleigh and Mie scattering). To extract the useful signal, the R-presentation of the spectrum intensity is carried out.[61−63]

$$R(\nu) = \frac{\nu \cdot (1 - e^{-h\nu/k^B T})}{(\nu_0 - \nu)^4} \cdot I(\nu)$$

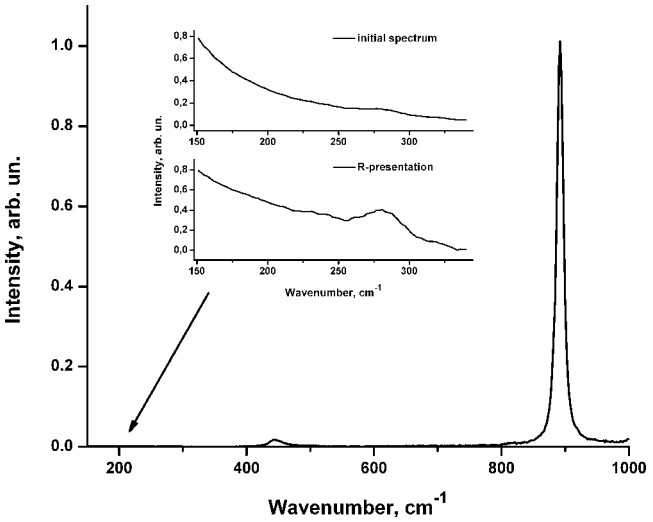

Figure 8. Low-frequency area of the Raman spectra of ethanol. The inset demonstrates the extraction of the useful signal from Raman spectrum using the R-presentation.

where ν_0 is the excitation frequency, ν is the Raman frequency shift, k^B is the Boltzmann constant, and T is the temperature. Using the R-presentation the intensities of Raman lines located at 270 and 886 cm^{-1} were found and the equilibrium constants for ethanol were calculated for different temperatures. Drawing the Van't Hoff plot and using the slope of its linear approximation, we determined the value of the enthalpy of formation/breaking the hydrogen bonds in ethanol $\Delta H^{Et} = -5.6$ kJ/mol. The error of the enthalpy calculation was 1.2 kJ/mol.

According to scientific publications the values of enthalpy of hydrogen bond formation in ethanol are varied from −4[53] to −10.5 kJ/mol.[60] Thus, the obtained value of the enthalpy of breaking hydrogen bonds in ethanol ΔH^{Et} we have received is a good agreement with literature data.

3.3. Appearance of Clathrate-like Structures in Raman Spectra of Water−Ethanol Solutions. We use the term "clathrate-like" to describe the network of water molecules with enhanced hydrogen bonding, which can be disrupted by kinetic effects (for example, raised temperature).

In Figure 9 the dependence of partial molar volumes V of ethanol and water on the mole fraction of ethanol x_{Et} (based on data of Moore[64] and the dependence of the enthalpy of formation/weakening of hydrogen bonds in water−ethanol mixtures on the mole fraction of ethanol x_{Et} are presented. Figure 9 shows the dependence of the partial molar volumes of ethanol and water on the mole fraction of ethanol. It can be seen that at ethanol mole fraction of around $x_{Et} = 0.07$ the molar volume of water has actually increased slightly compared to that of the pure liquid, whereas that of ethanol reaches a minimum. This means that ethanol molecules occupy less volume (i.e., they are more densely packed) at a concentration of about $x_{Et} = 0.07$, and the water density decreases at the $x_{Et} = 0.07$ (which corresponds to a concentration of 20 vol %). Equally at high ethanol mole fraction, the ethanol partial molar volume approaches its pure liquid value, whereas that of water has fallen significantly below its pure liquid value, reaching a minimum around $x_{Et} = 0.85$. It is possible that the decrease in partial molar volume of either component occurs when dilution arises due to their inability to form structures with neighboring molecules of the same kind. Thus, the presented dependences

DOI: 10.1021/acs.jpca.5b06678
J. Phys. Chem. A XXXX, XXX, XXX−XXX

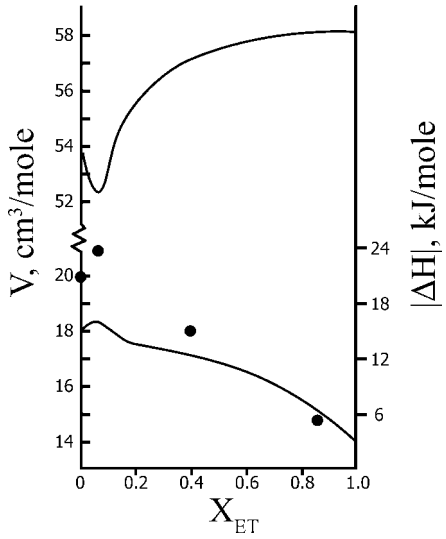

Figure 9. Dependence of partial molar volumes V of ethanol (upper curve) and water (low curve) as functions of mole fraction of ethanol x_{Et} at 25 °C and 1 bar (based on data of Moore[64] (left axis, solid curve) and the dependence of the enthalpy of formation/weakening of hydrogen bonds in water−ethanol mixtures on the mole fraction of ethanol x_{Et} (right axis, dots).

indicate the possible existence of clathrate-like structures in water−ethanol solutions.

The comparison of all calculated values of the enthalpy of formation/weakening of the hydrogen bonds in water, in aqueous ethanol solutions with x_{Et} = 0.07 (20 vol %) and x_{Et} = 0.39 (70 vol %) of ethanol, and in x_{Et} = 0.85 (96 vol %) ethanol (Figure 10) shows that the strongest hydrogen bonds are

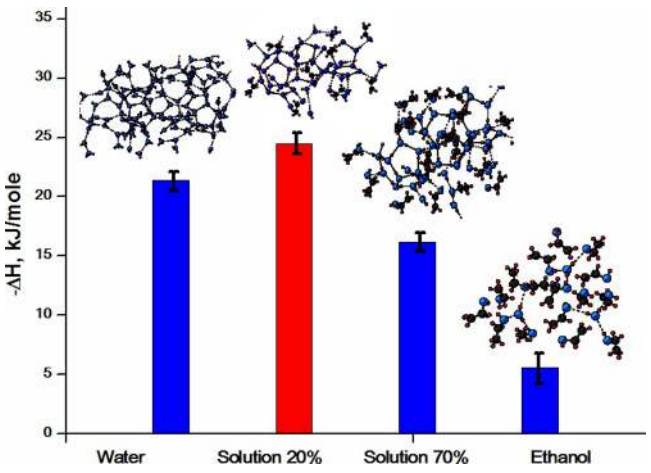

Figure 10. Enthalpy of formation/weakening of hydrogen bonds in water, ethanol, and their mixtures.

formed within the ethanol hydrates in the 20 vol % ethanol solution. At this concentration, the hydrogen bonds on average are stronger than that in pure water. These results once again confirm the hypothesis of the existence of clathrate-like structures with strong hydrogen bonding in water−ethanol solutions at an ethanol concentration of 20 vol %.

4. CONCLUSIONS

In this work the Raman spectra of water, ethanol, and water−ethanol solutions with 20 and 70 vol % of ethanol were measured and analyzed under temperature ranging from −10 to +70 °C. Application of the MCR-ALS method allowed extracting contributions of molecules with different strengths of hydrogen bonding into the OH stretching band 3000−3800 cm^{-1}. This, in turn, allowed determining the molar ratio of molecules with strong and weak hydrogen bonding in the wide range of temperatures. Using the Van't Hoff plot, the enthalpies of formation/weakening of hydrogen bonds were calculated for each of the studied liquid samples: ΔH^{w} = −21.4 ± 0.7 kJ/mol, $\Delta H^{20\%}$ = −24.5 ± 0.8 kJ/mol, $\Delta H^{70\%}$ = −16.2 ± 0.8 kJ/mol, and ΔH^{Et} = −5.6 ± 1.2 kJ/mol. We are not aware of other studies in which the values of the energy (enthalpy) of formation/weakening of hydrogen bonds in ethanol hydrates in solutions with various ethanol concentrations were determined.

The calculations showed that the energy (enthalpy) of formation/weakening of hydrogen bonds was the highest among all the samples in an aqueous solution with 20 vol % of ethanol. This indicates the strengthening of hydrogen bonds between OH groups of water molecules and between molecules of water and ethanol in the ethanol hydrates. Thus, our findings corroborate other experimental evidence of clathrate-like structures in water−ethanol solutions with concentrations around 20 vol % of ethanol (ethanol mole fraction x_{Et} = 0.07).

■ ASSOCIATED CONTENT

Supporting Information

The Supporting Information is available free of charge on the ACS Publications website at DOI: 10.1021/acs.jpca.5b06678.

Figure S1 shows the polarized Raman spectra of 70 vol % water−ethanol solution at different temperatures. Figure S2 shows the Raman spectrum for 20 vol % ethanol solution at temperature 0 °C (Figure S2a), at temperature 15.4 °C (Figure S2b), and at temperature 20.4 °C (Figure S2c) and its decomposition into 4 individual components by MCR-ALS method. Figures S3 shows the Raman spectrum for 70 vol % ethanol solution at temperature 9.3 °C (Figure S3a), at temperature 20.4 °C (Figure S3b), and at temperature 69.2 °C (Figure S3c) and its decomposition into four individual components by the MCR-ALS method. Figure S4 shows the linearity of the Van't-Hoff's plots for water (a), for the water−ethanol solutions with ethanol content 20 vol % (b) and 70 vol % (c), and for ethanol (d) (PDF)

■ AUTHOR INFORMATION

Corresponding Author

*T. Dolenko. E-mail: tdolenko@lid.phys.msu.ru, tdolenko@mail.ru. Phone: +7 (495) 939 1653.

Notes

The authors declare no competing financial interest.

■ ACKNOWLEDGMENTS

This study was supported by the Russian Scientific Foundation, grant no. 14-11-00579.

■ REFERENCES

(1) Matsugami, M.; Yamamoto, R.; Kumai, T.; Tanaka, M.; Umecky, T.; Takamuku, T. Hydrogen Bonding in Ethanol−Water and Trifluoroethanol−Water Mixtures Studied by NMR and Molecular Dynamics Simulation. *J. Mol. Liq.* **2015**.

(2) Li, R.; D'Agostino, C.; McGregor, J.; Mantle, M. D.; Zeitler, J. A.; Gladden, L. F. Mesoscopic Structuring and Dynamics of Alcohol/

DOI: 10.1021/acs.jpca.5b06678
J. Phys. Chem. A XXXX, XXX, XXX−XXX

Water Solutions Probed by Terahertz Time-Domain Spectroscopy and Pulsed Field Gradient Nuclear Magnetic Resonance. *J. Phys. Chem. B* **2014**, *118* (34), 10156−10166.
(3) Asenbaum, A.; Pruner, C.; Wilhelm, E.; Mijakovic, M.; Zoranic, L.; Sokolic, F.; Kezic, B.; Perera, A. Structural Changes in Ethanol−Water Mixtures: Ultrasonics, Brillouin Scattering and Molecular Dynamics Studies. *Vib. Spectrosc.* **2012**, *60*, 102−106.
(4) Nedić, M.; Wassermann, T. N.; Larsen, R. W.; Suhm, M. A. A Combined Raman- and Infrared Jet Study of Mixed Methanol−Water and Ethanol−Water Clusters. *Phys. Chem. Chem. Phys.* **2011**, *13*, 14050−14063.
(5) Pradhan, T.; Ghoshal, P.; Biswas, R. Structural Transition in Alcohol-Water Binary Mixtures: A Spectroscopic Study. *Proc. - Indian Acad. Sci., Chem. Sci.* **2008**, *120* (2), 275−287.
(6) Dixit, S.; Crain, J.; Poon, W. C. K.; Finney, J. L.; Soper, A. K. Molecular Segregation Observed in a Concentrated Alcohol-Water Solution. *Nature* **2002**, *416* (6883), 829−832.
(7) Guo, J.-H.; Luo, Y.; Augustsson, A.; Kashtanov, S.; Rubensson, J.-E.; Shuh, D. K.; Agren, H.; Nordgren, J. Molecular Structure of Alcohol-Water Mixtures. *Phys. Rev. Lett.* **2003**, *91*, 157401.
(8) Ageev, D. V.; Patsaeva, S. V.; Ryzhikov, B. D.; Yuzhakov, V. I.; Sorokin, V. N. Influence of Temperature and Ethanol Content on Aggregation of Rhodamine 6G Molecules in Aqueous Ethanol Solutions. *J. Appl. Spectrosc.* **2008**, *75* (5), 653−657.
(9) D'Angelo, M.; Onori, G.; Santucci, A. Self-Association of Monohydric Alcohols in Water: Compresibility and Infrared Absorption Measurements. *J. Chem. Phys.* **1994**, *100*, 3107−3113.
(10) Onori, G.; Santucci, A. Dynamical and Structural Properties of Water/Alcohol Mixtures. *J. Mol. Liq.* **1996**, *69*, 161−181.
(11) Nakanishi, K.; Kato, N.; Maruyama, M. Excess and Partial Volumes of Some Alcohol-Water and Glycol-Water Solutions. *J. Phys. Chem.* **1967**, *71*, 814−818.
(12) Schott, H. Hydration of Primary Alcohols. *J. Chem. Eng. Data* **1969**, *14*, 237−239.
(13) McGlashan, M. L.; Williamson, A. G. Isothermal Liquid Vapor Equilibria for System Methanol-Water. *J. Chem. Eng. Data* **1976**, *21*, 196−199.
(14) Petong, P.; Pottel, R.; Kaatze, U. Water - Ethanol Mixtures at Different Compositions and Temperatures. A Dieletric Relaxation Study. *J. Phys. Chem. A* **2000**, *104*, 7420−7428.
(15) Koga, Y.; Nishikawa, K.; Westh, P. ″Icebergs″ or No ″Icebergs″ in Aqueous Alcohols?: Composition-Dependent Mixing Schemes. *J. Phys. Chem. A* **2004**, *108* (17), 3873−3877.
(16) Sato, T.; Chiba, A.; Nozaki, R. Dynamical Aspects of Mixing Schemes in Ethanol-Water Mixtures in Terms of the Excess Partial Molar Activation Free Energy, Enthalpy, and Entropy of the Dielectric Relaxation Process. *J. Chem. Phys.* **1999**, *110* (5), 2508−2521.
(17) Nishikawa, K.; Iijima, T. Small-angle X-ray Scattering Study of Fluctuations in Ethanol and Water Mixtures. *J. Phys. Chem.* **1993**, *97* (41), 10824−10828.
(18) Wakisaka, A.; Matsuura, K. Microheterogeneity of Ethanol-Water Binary Mixtures Observed at the Cluster Level. *J. Mol. Liq.* **2006**, *129* (1−2), 25−32.
(19) Soper, A. K.; Dougan, L.; Crain, J.; Finney, J. L. Excess Entropy in Alcohol−Water Solutions: A Simple Clustering Explanation. *J. Phys. Chem. B* **2006**, *110* (8), 3472−3476.
(20) Dougan, L.; Crain, J.; Finney, J. L.; Soper, A. K. Molecular Self-Assembly in a Model Amphiphile System. *Phys. Chem. Chem. Phys.* **2010**, *12*, 10221−10229.
(21) Murthy, S. S. N. Detailed Study of Ice Clathrate Relaxation: Evidence for the Existence of Clathrate Structures in Some Water-Alcohol Mixtures. *J. Phys. Chem. A* **1999**, *103*, 7927−7937.
(22) Alavi, S.; Takeya, S.; Ohmura, R.; Woo, T. K.; Ripmeester, J. A. Hydrogen-Bonding Alcohol-Water Interactions in Binary Ethanol, 1-Propanol, and 2-Propanol+Methane Structure II Clathrate Hydrates. *J. Chem. Phys.* **2010**, *133* (7), 074505.
(23) Allison, S. K.; Fox, J. P.; Hargreaves, R.; Bates, S. P. Clustering and Microimmiscibility in Alcohol-Water Mixtures: Evidence from Molecular-Dynamics Simulations. *Phys. Rev. B: Condens. Matter Mater. Phys.* **2005**, *71* (2), 024201.
(24) Yang, D.; Wang, H. Effects of Hydrogen Bonding on the Transition Properties of Ethanol−Water Clusters: A TD-DFT Study. *J. Cluster Sci.* **2013**, *24*, 485−495.
(25) Banerjee, S.; Ghosh, R.; Bagchi, B. Structural Transformations, Composition Anomalies and Dramatic Collapse of Linear Polymer Chains in Dilute Ethanol - Water Mixtures. *J. Phys. Chem. B* **2012**, *116*, 3713−3722.
(26) Fileti, E. E.; Chaudhuri, P.; Canuto, S. Relative Strength of Hydrogen Bond Interaction in Alcohol−Water Complexes. *Chem. Phys. Lett.* **2004**, *400*, 494−499.
(27) Noskov, S.; Lamoureux, G.; Roux, B. Molecular Dynamics Study of Hydration in Ethanol-Water Mixtures Using a Polarizable Force Field. *J. Phys. Chem. B* **2005**, *109*, 6705−6713.
(28) Zhang, C.; Yang, X. Molecular Dynamics Simulation of Ethanol/Water Mixtures for Structure and Diffusion Properties. *Fluid Phase Equilib.* **2005**, *231*, 1−10.
(29) Mizuno, K.; Miyashita, Y.; Shindo, Y.; Ogawa, H. NMR and FT-IR Studies of Hydrogen Bonds in Ethanol-Water Mixtures. *J. Phys. Chem.* **1995**, *99* (10), 3225−3228.
(30) Nose, A.; Hojo, M. Hydrogen Bonding of Water−Ethanol in Alcoholic Beverages. *J. Biosci. Bioeng.* **2006**, *102* (4), 269−280.
(31) Parke, S. A.; Birch, G. G. Solution Properties of Ethanol in Water. *Food Chem.* **1999**, *67* (3), 241−246.
(32) Czarnecki, M. A.; Wojtków, D. Effect of Varying Water Content on the Structure of Butyl Alcohol/Water Mixtures: FT-NIR Two-Dimensional Correlation and Chemometric Studies. *J. Mol. Struct.* **2008**, *883*−*884*, 203−208.
(33) Matsumoto, M.; Nishi, N.; Furusawa, T.; Saita, M.; Takamuku, T.; Yamagami, M.; Yamaguchi, T. Structure of Clusters in Ethanol-Water Binary Solutions Studied by Mass Spectrometry and X-Ray Diffraction. *Bull. Chem. Soc. Jpn.* **1995**, *68*, 1775−1783.
(34) Egashira, K.; Nishi, N. Low-Frequency Raman Spectroscopy of Ethanol-Water Binary Solution: Evidence for Self-Association of Solute and Solvent Molecules. *J. Phys. Chem. B* **1998**, *102* (21), 4054−4057.
(35) Ahmed, M. K.; Ali, S.; Wojcik, E. The C-O Stretching Infrared Band as a Probe of Hydrogen bonding in ethanol-water and methanol-water mixtures. *Spectrosc. Lett.* **2012**, *45*, 420−423.
(36) Nishi, N.; Takahashi, S.; Matsumoto, M.; Tanaka, A.; Muraya, K.; Takamuku, T.; Yamaguchi, T. Hydrogen-Bonded Cluster Formation and Hydrophobic Solute Association in Aqueous Solutions of Ethanol. *J. Phys. Chem.* **1995**, *99* (1), 462−468.
(37) Takamuku, T.; Saisho, K.; Nozawa, S.; Yamaguchi, T. X-ray Diffraction Studies on Methanol-Water, Ethanol-Water, and 2-Propanol-Water Mixtures at Low Temperatures. *J. Mol. Liq.* **2005**, *119* (1−3), 133−146.
(38) Juurinen, I.; Nakahara, K.; Ando, N.; Nishiumi, T.; Seta, H.; Yoshida, N.; Morinaga, T.; Itou, M.; Ninomiya, T.; Sakurai, Y.; et al. Measurement of Two Solvation Regimes in Water-Ethanol Mixtures Using X-Ray Compton Scattering. *Phys. Rev. Lett.* **2011**, *107* (5), 197401.
(39) Burikov, S.; Dolenko, T.; Patsaeva, S.; Starokurov, Yu.; Yuzhakov, V. Raman and IR Spectroscopy Research on Hydrogen Bonding in Water-Ethanol Systems. *Mol. Phys.* **2010**, *108* (18), 2427−2436.
(40) Hu, N.; Wu, D.; Cross, K.; Burikov, S.; Dolenko, T.; Patsaeva, S.; Schaefer, D. W. Structurability: A Collective Measure of the Structural Differences in Vodkas. *J. Agric. Food Chem.* **2010**, *58* (12), 7394−7401.
(41) Burikov, S.; Dolenko, S.; Dolenko, T.; Patsaeva, S.; Yuzhakov, V. Decomposition of Water Raman Stretching Band with a Combination of Optimization Methods. *Mol. Phys.* **2010**, *108* (6), 739−747.
(42) Dolenko, T. A.; Burikov, S. A.; Patsaeva, S. V.; Yuzhakov, V. I. Manifestation of Hydrogen Bonds of Aqueous Ethanol Solutions in the Raman Scattering Spectra. *Quantum Electron.* **2011**, *41* (3), 267−272.
(43) Schicks, J. M.; Erzinger, J.; Ziemann, M. A. Raman Spectra of Gas Hydrates–Differences and Analogies to Ice 1h and (Gas

DOI: 10.1021/acs.jpca.5b06678
J. Phys. Chem. A XXXX, XXX, XXX−XXX

Saturated) Water. *Spectrochim. Acta, Part A* **2005**, *61* (10), 2399−2403.
(44) Tauler, R.; de Juan, A. *Multivariate Curve Resolution − Alternating Least-Squares (MCR-ALS)*; MatLab Code, University of Barcelona, 1999.
(45) de Juan, A.; Tauler, R. Multivariate Curve Resolution (MCR) from 2000: Progress in Concepts and Applications. *Crit. Rev. Anal. Chem.* **2006**, *36*, 163−176.
(46) Zhang, X.; Tauler, R. Application of Multivariate Curve Resolution Alternating Least Squares (MCR-ALS) to Remote Sensing Hyperspectral Imaging. *Anal. Chim. Acta* **2013**, *762*, 25−38.
(47) Dolenko, T. A.; Burikov, S. A.; Dolenko, S. A.; Efitorov, A. O.; Mirgorod, Y. A. Raman Spectroscopy of Micellization-Induced Liquid-Liquid Fluctuations in Sodium Dodecyl Sulfate Aqueous Solutions. *J. Mol. Liq.* **2015**, *204*, 44−49.
(48) Goldberg, D. E. *Genetic Algorithms in Search, Optimization, and Machine Learning*; Addison-Wesley Publishing Co.: Reading, MA, 1989.
(49) Walrafen, G. E. Raman Spectral Studies of the Effects of Temperature on Water Structure. *J. Chem. Phys.* **1967**, *47* (1), 114−126.
(50) Gerdova, I. V.; Dolenko, S. A.; Dolenko, T. A.; Churina, I. V.; Fadeev, V. V. New Opportunity Solutions to Inverse Problems in Laser Spectroscopy Involving Artificial Neural Networks. *Izv. Akad. Nauk, Ser. Fiz.* **2002**, *66* (8), 1116−1124.
(51) Chaplin, M. Water Structure and Behavior. www.lsbu.ac.uk/water.
(52) Dolenko, T. A.; Churina, I. V.; Fadeev, V. V.; Glushkov, S. M. Valence Band of Liquid Water Raman Scattering: Some Peculiarities and Applications in the Diagnostics of Water Media. *J. Raman Spectrosc.* **2000**, *31* (8−9), 863−870.
(53) Moskva, V. V. Hydrogen Bond in Organic Chemistry. *Soros Educational Journal* **1999**, *2*, 58−64.
(54) Chaplin, M. Water's Hydrogen Bond Strength. Eprint arXiv:0706.1355 [cond-mat.soft], 10 Jun 2007, 20 pp.
(55) Suresh, S. J.; Naik, V. M. Hydrogen Bond Thermodynamic Properties of Water from Dielectric Constant Data. *J. Chem. Phys.* **2000**, *113*, 9727−9732.
(56) Khan, A. A Liquid Water Model: Density Variation from Supercooled to Superheated States, Prediction of H-bonds, and Temperature Limits. *J. Phys. Chem. B* **2000**, *104*, 11268−11274.
(57) Stokely, K.; Mazza, M. G.; Stanley, H. E.; Franzese, G. Effect of Hydrogen Bond Cooperativity on the Behavior of Water. *Proc. Natl. Acad. Sci. U. S. A.* **2010**, *107* (4), 1301−1306.
(58) Smith, J. D.; Cappa, C. D.; Wilson, K. R.; Messer, B. M.; Cohen, R. C.; Saykally, R. J. Energetics of Hydrogen Bond Network Rearrangements in Liquid Water. *Science* **2004**, *306*, 851−853.
(59) Chumaevskii, N. A.; Rodnikova, M. N. Some Peculiarities of Liquid Water Structure. *J. Mol. Liq.* **2003**, *106*, 167−177.
(60) Edwards, H. G. M.; Farwell, D. W.; Jones, A. A. Quantitative Raman Spectroscopic Investigation of Hydrogen-Bonding in Ethanol and Ethanol-d_1. *Spectrochim. Acta* **1989**, *45A* (11), 1165−1171.
(61) Nielsen, O. V.; Lund, P. A.; Praestgaard, E. Low-Frequency Vibrations (20−400 cm^{-1}) of Some Mononucleosides in Aqueous Solution. *J. Raman Spectrosc.* **1980**, *9* (5), 286−290.
(62) Brooker, M. H.; Nielsen, O. F.; Praestgaard, E. Assessment of Correction Procedures for Reduction of Raman Spectra. *J. Raman Spectrosc.* **1988**, *19*, 71−78.
(63) Nielsen, O. F. The Structure of Liquid Water. Low Frequency (10−400 cm^{-1}) Raman Study. *Chem. Phys. Lett.* **1979**, *60* (3), 515−517.
(64) Moore, W. J. *Physical Chemistry*, 4th ed.; Prentice-Hall: Englewood Cliffs, NJ, 1972.

DOI: 10.1021/acs.jpca.5b06678
J. Phys. Chem. A XXXX, XXX, XXX−XXX